

Journal of Materials Chemistry B

Accepted Manuscript



This is an *Accepted Manuscript*, which has been through the Royal Society of Chemistry peer review process and has been accepted for publication.

Accepted Manuscripts are published online shortly after acceptance, before technical editing, formatting and proof reading. Using this free service, authors can make their results available to the community, in citable form, before we publish the edited article. We will replace this *Accepted Manuscript* with the edited and formatted *Advance Article* as soon as it is available.

You can find more information about *Accepted Manuscripts* in the [Information for Authors](#).

Please note that technical editing may introduce minor changes to the text and/or graphics, which may alter content. The journal's standard [Terms & Conditions](#) and the [Ethical guidelines](#) still apply. In no event shall the Royal Society of Chemistry be held responsible for any errors or omissions in this *Accepted Manuscript* or any consequences arising from the use of any information it contains.



Journal Name

COMMUNICATION

Virus-inspired mimics: self-assembly of dendritic lipopeptides into arginine-rich nanovectors for improving gene delivery

Received 00th January 20xx,
Accepted 00th January 20xx

Xianghui Xu, Qian Jiang, Xiao Zhang, Yu Nie*, Zhijun Zhang, Yunkun Li, Gang Cheng, Zhongwei Gu*

DOI: 10.1039/x0xx00000x

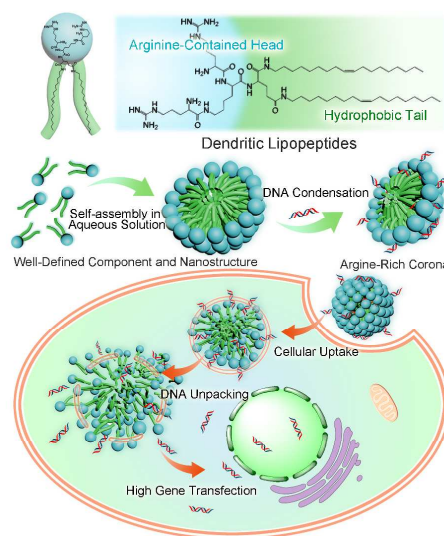
www.rsc.org/

With inspirations from natural viruses, the arginine-containing dendritic lipopeptides were designed for bioinspired fabrication. Self-assembling the defined amphiphilic lipopeptides generated virus-inspired nanovectors with the arginine-rich corona. These nanovectors provided some remarkable benefits for gene delivery, including well-defined nanostructure, high transfection efficiency, serum resistance and low cytotoxicity.

Over the past decade, bio-inspirations learned from Mother Nature have a profound impact on the development of novel material systems, such as highly-tough hybrid materials and bioinspired surfaces with special wettability.^{1, 2} High infectivity of natural viruses inspires scientist to fabricate virus-based vectors for gene delivery; and virus-based vectors have gained large success in gene therapy for various diseases (for example, “Gendicine” as the first gene medicine approved for clinical use in humans).³ With the increasing number of adverse events (e.g., mutagenesis and immunogenicity) caused by virus-based vectors in clinical trials,⁴ more and more attentions were paid to developing non-viral vectors for efficient and safe gene delivery.⁵⁻⁸ However, many shortages of non-viral vectors, such as poor efficiency and high cytotoxicity, still need to be overcome for further applications.^{9, 10} It is reasonable to predict that integrating the advantages of artificial vectors with viral inspirations will become a new strategy for obtaining ideal gene vectors.¹¹

Some of the latest attempts on developing gene vectors focus on mimicking key features of natural viruses; meanwhile, the structural and functional mimics of viruses largely promote gene transfection efficiency.¹¹ Notably, both molecular science and supramolecular science play an important role in the development of new virus-inspired nanomaterials. On one hand, high infectivity of virus-based vectors largely depends on the highly bioactive molecules, such as cell penetrating peptides (CPPs).¹² For example, synthetic arginine-rich molecules mimicking CPPs greatly improved cell penetration

and gene delivery.¹³ We simulated the viral components by the arginine-functionalized polysaccharides to protect nucleic acid against DNase degradation and enhance delivery efficiency.¹⁴ On the other hand, supramolecular self-assembly provide a convenient approach to mimic the viral architectures and functions;¹⁵ and some supramolecular viral mimics indeed enhanced delivery efficiency of gene and drug.^{16, 17} We also reported a supramolecular strategy on the self-assembly globulin-like peptide dendrimers into artificial capsids generating high delivery efficiency;^{18, 19} very recently, we successfully developed arginine-rich nanohybrids for highly efficient gene delivery and biological imaging by supramolecular hybrid self-assembly.²⁰ As our continuous interests in the research of virus-inspired nanomaterials for therapeutic delivery, we think current virus-inspired vectors still have lots of requirements to be improved for in-depth studies, such as more viral inspirations, higher delivery efficiency, defined and safe components, facile manufacture and low cost.



Scheme 1 Graphic illustration for dendritic lipopeptides, virus-inspired nanovectors self-assembled from amphiphilic lipopeptides and their intracellular gene delivery.

National Engineering Research Center for Biomaterials, Sichuan University, 29 Wangjiang Road, Chengdu, Sichuan 610064, China.
E-mail: zwgu@scu.edu.cn (Z. Gu), nie_yu@scu.edu.cn (Y. Nie).
Fax: +86 28-85410653; Tel: +86 28-85414308
† Electronic supplementary information (ESI) available. See DOI: XXXXXXXXXXXXX

Herein, we would like to demonstrate a rational and facile design of virus-inspired nanovectors for efficient gene delivery, and the following viral inspirations are elaborately involved into this system: (i) inspired by the viral components, defined lipopeptides are engineered as bioinspired building blocks;²¹ (ii) inspired by the viral architectures for nucleic acid packing, self-assembly of amphiphilic dendritic molecules are designed for mimicking the nanostructure of viral envelopes or capsids;¹⁵ (iii) based on the molecular design and supramolecular self-assembly, fabricating arginine-rich corona to mimic bioactivity of viral cell penetrating peptides (e.g., TAT).¹² We expect that this type of virus-inspired nanovectors will hold the features of high delivery efficiency, low cytotoxicity and facile manufacture for clinical application.

The designed chemical structure of dendritic lipopeptides is shown in **Scheme 1**, and they can be synthesized with a defined molecular structure through a facile synthesis.^{22, 23} In brief, amino groups in lysine were conjugated with arginine to generate arginine-containing segments; and both carboxyl groups in glutamic acid were modified with oleylamine as hydrophobic tails. Then the arginine-containing segments and the dual hydrophobic tails were linked together by covalent bond. After removal of protections in amino groups and guanidine groups, the amphiphilic dendritic lipopeptides (DLPs) were obtained with the arginine-containing peptide as hydrophilic head and the dual-tail lipids as hydrophobic tails. The result of matrix-assisted laser desorption/ionization time-of-flight mass spectrometry (MALDI-TOF MS) provided a direct evidence to confirm that DLPs was obtained with a defined structure ($[M+H]^+ = 1086.98$, observed in **Fig. 1A**), which was consistent with the calculated value ($[M+H]^+ = 1086.92$). The detailed synthetic routes and characterizations of each compound can be found in the ESI†.

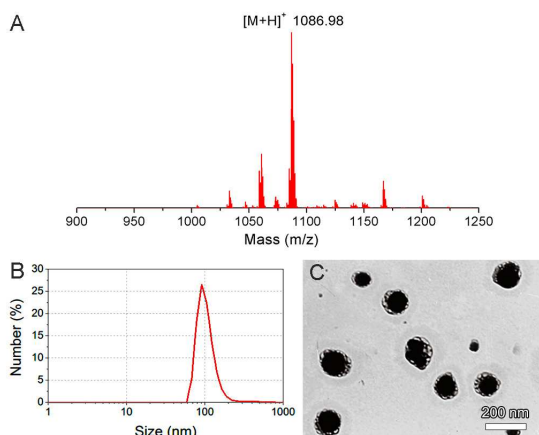


Fig. 1 (A) MALDI-TOF mass spectrum of dendritic lipopeptides, MS (m/z , $[M+H]^+$): 1086.98 (observed), 1086.92 (calculated); (B) size distribution (in aqueous solution) and (C) TEM image of AVNs.

Next, we drove the self-assembly of DLPs into available vectors in aqueous solution as shown in **Scheme 1**. Dynamic light scattering (DLS) measurement indicated DLPs can self-assemble into arginine-rich virus-inspired nanovectors (AVNs) with an average size of about 110 nm (**Fig. 1B**). As shown by transmission electron microscopy

(TEM), AVNs presented a well-defined spherical shape of approximately 120 nm diameter (**Fig. 1C**). The scanning electron microscope (SEM) image and atomic force microscope (AFM) image agreed very well with the results (**Fig. S7** in ESI†). More importantly, zeta potential of AVNs reached up to 41.1 ± 0.12 mV ($n = 3$) in aqueous solution, which proved the formation of arginine-rich corona with abundant amino groups and guanidine groups.

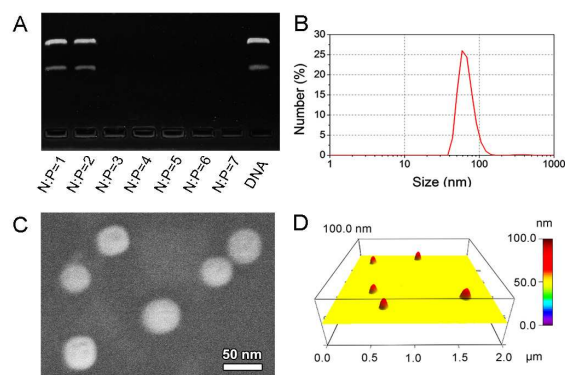


Fig. 2 (A) Agarose gel electrophoresis of DNA/AVNs complex at different N/P ratio. (B) Size distribution (in aqueous solution), (C) SEM and (D) AFM image of DNA-packaged AVNs at the N/P ratio of 20.

The binding ability of AVNs with DNA was determined by agarose gel retention assay. In **Fig. 2A**, the DNA mobility in the AVNs/DNA complex was completely retarded at the N/P ratio of 3. When these AVNs condensed with pDNA at the N/P ratio of 20, approximately 40% size reduction was observed in DLS result (about 70 nm, **Fig. 2B**), while DNA-packaged AVNs kept the similar zeta potential (41.5 ± 1.82 mV, $n = 3$) as primary AVNs. It can be speculated that the negatively-charged DNA were mainly embed into the arginine-rich corona for the following reasons: (i) inserted DNA reduced the charge repulsion among the arginine-rich corona and strengthened the electrostatic interaction of the whole system, and further resulted in more compact nanostructure; (ii) no change on the zeta potential also suggested loaded DNA might not locate on the surface of AVNs but insert into the arginine-rich corona.²⁴ The scanning electron microscopy (SEM) image showed the well-defined nanostructure of DNA-packaged AVNs with about 50 nm in size (**Fig. 2C**). In addition, atomic force microscopy (AFM) clearly illustrated three dimensional (3D) architectures of DNA-packaged AVNs, which were in good agreement with TEM and DLS results (**Fig. 2D**). These results revealed that this virus-inspired strategy was able to fabricate virus-like mimics with compact nanostructure and arginine-rich corona.

Once the formation of DNA-packaged AVNs was confirmed, we turn to investigate their utility for gene delivery to tumor cell lines. The gene transfection of DNA-packaged AVNs containing pEGFP-C1 and pGL3-Luc were first carried out on a human hepatocellular carcinoma HepG2 cell line. Polyethyleneimine (PEI) was as a positive control in this study, because of its highly-efficient gene transfection without fetal bovine serum (FBS), regarding as a golden standard.^{25, 26} In the absence of FBS, green fluorescent protein (GFP) expression in the AVNs group at N/P ratio of 40 was much stronger than positive control of the PEI group (**Fig. 3A**). However,

in the culture medium containing 10% FBS mimicking normal physiological condition, GFP expression in PEI group reduced significantly, which are drawbacks of typical cationic polymers.¹⁰ Encouragingly, pEGFP-packaged AVNs still kept high GFP expression in HepG2 cells with 10% FBS. Without FBS, the quantitative results showed luciferase expression mediated by AVNs (N/P = 40) was about 5-fold higher than that of PEI (Fig. 3B). Moreover, the efficiency of pGL3-Luc transfection (3.43×10^9 RLU/mg of protein, N/P 40) in the AVNs group with 10% FBS was still comparable to that of the positive control group (3.07×10^9 RLU/mg of protein, PEI group without FBS, N/P 10).

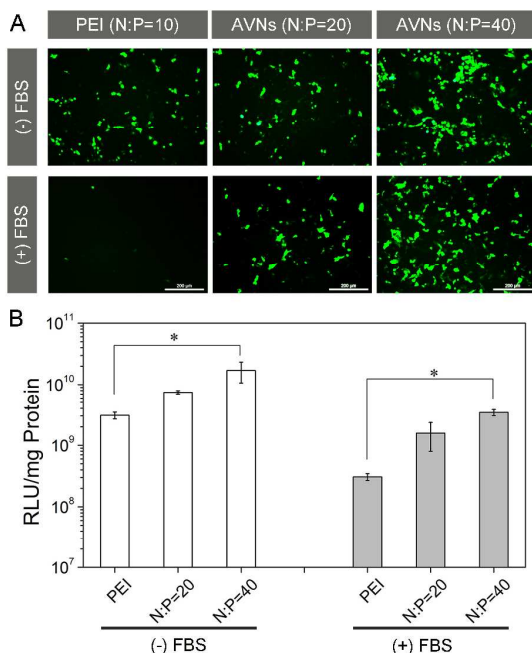


Fig 3. (A) GFP expression in HepG2 tumor cells after exposure to the PEI/pEGFP-C1 complex and the AVNs/pEGFP-C1 complex without (-) FBS and with (+) FBS for 48 hours. (B) Luciferase gene transfection in HepG2 cells after exposure to the PEI/pGL3-Luc complex and the AVNs/pGL3-Luc complex without (white) and with (grey) FBS for 48 hours (* $p < 0.01$, $n = 6$).

As promising vectors for gene therapy, they often should hold universal potentials of efficient gene delivery to various tumor cell lines. As a result, gene transfection efficiency of AVNs was also performed on other tumor cell lines, including murine melanoma cells B16F10 (Fig. S9 and Fig. S10 in ESI[†]) and human breast cancer cells MCF7 (Fig. S11 and Fig. S12 in ESI[†]). Within the culture medium containing 10% FBS, the qualitative and quantitative results consistently confirmed AVNs held much higher transfection efficiency than PEI. Taken together, the virus-inspired nanovectors provided some most important features for gene delivery, including high delivery efficiency to various tumor cell lines and excellent serum resistance.

Motivated by the high transfection efficiency of the DNA-packaged AVNs, we further investigated their intracellular fate using fluorescence activated cell sorting (FACS) and confocal laser scanning microscope (CLSM).²⁷ AVNs and PEI were labeled with

fluorescein isothiocyanate (FITC), and DNA was labeled with Cy5. For qualitative and quantitative analysis, DNA concentration and the fluorescence labeled amount of nanovectors were adjusted at the same level. As shown in Fig. 4A, DNA-packaged AVNs obviously facilitated internalization compared DNA-packaged PEI within 1.5 h. CLSM images indicated that DNA-packaged AVNs were internalized into HepG2 cells and dispersed in the cytoplasm with 2.5 hours (Fig. S14 and Fig. S15). More importantly, when the incubation time was increased to 5.0 hours, a part of Cy5-labeled DNA in AVNs group was released from AVNs and delivered into the nucleus region in HepG2 tumor cells (Fig. 4B). In contrast, most of DNA was still aggregated together or associated with the PEI in the cytoplasm. As expected, supramolecular arginine-rich corona enhanced cellular uptake of the DNA-packaged AVNs, and the supramolecular AVNs assembled from small dendritic lipopeptides were more beneficial to disassembly and DNA release in the cytosol, distinguishing from the covalent macromolecules of PEI.

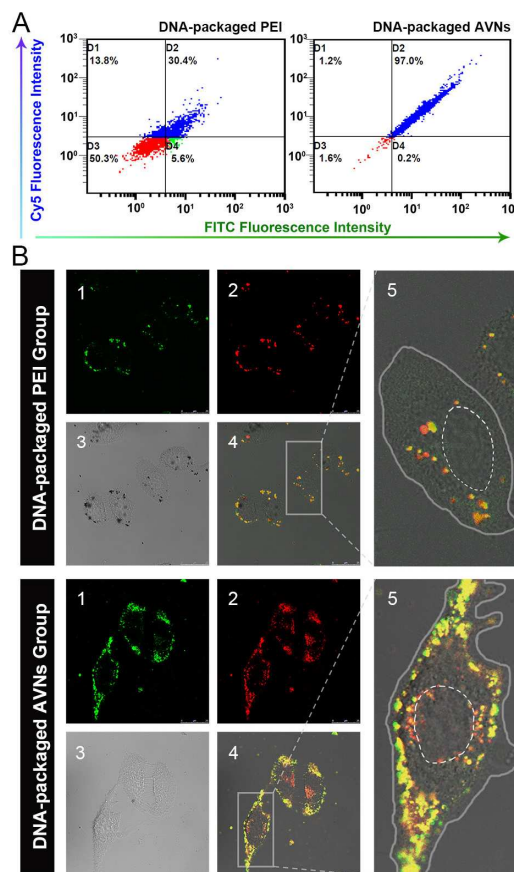


Fig 4. (A) Flow cytometry analysis of HepG2 cells after incubation with fluorescence labelled DNA-packaged PEI and DNA-packaged AVNs for 1.5 h with FBS. (B) CLSM images for intracellular delivery of the fluorescence labelled DNA-packaged PEI and DNA-packaged AVNs in HepG2 cells for 5.0 h, including FITC channel (1), Cy5 channel (2), bright field (3), overlay (4), and enlarged view (5).

Cytotoxicity is an important consideration for available gene vectors.¹⁰ Therefore, cell counting kit-8 (CCK-8) assay was used to evaluate the cytotoxicity of the DNA-packaged AVNs and PEI/DNA

complex against HepG2 cells. The DNA-packaged AVNs showed no obvious cytotoxicity to HepG2 cells at a wide range of N/P 10 to N/P 80, while the PEI/DNA complex with high transfection efficiency caused significant cytotoxicity (~70% cell viability) owing to the innate drawback of cationic polymers (Fig. 5A).²⁸ Even if the PEI/DNA complex showed low cytotoxicity to HepG2 cells with FBS, the complex caused serious apoptosis. Fluorescence images showed a large number of apoptotic cells in the PEI group were stained by propidium iodide (PI), but few apoptotic cells were found in the AVNs group (Fig. 5B).²⁹ In the merged image of fluorescence and bright field, all of PI-stained cells accompanied with remarkable shrinkage of nuclei. As expected, the AVNs/DNA complexes at N/P ratio from 10 to 80 were obviously nontoxic to cells, and the AVNs group didn't induce cell apoptosis. Therefore, AVNs overcome the high cytotoxicity of typical cationic vectors for gene delivery.

in vitro gene therapy. We hope that self-assembly of bioinspired building blocks will become a new trend of building novel vectors for biomedical applications.

Acknowledgements

This work was supported by National Natural Science Foundation of China (NSFC, 51133004, 81361140343 and 31271020), National Basic Research Program of China (973 program, 2011CB606206), Joint Sino-German Research Project (GZ756 and GZ905), Sichuan Province Science and Technology Support Program (2013FZ0003, 2015SZ0122 and 2015SZ0189), Scientific Research Foundation for Talent Introduction (YJ201463) and Youth Scholars (2015SCU11037) from Sichuan University.

Notes and references

1. E. Munch, M. E. Launey, D. H. Alsem, E. Saiz, A. P. Tomsia and R. O. Ritchie, *Science*, 2008, **322**, 1516-1520.
2. K. Liu, X. Yao and L. Jiang, *Chem. Soc. Rev.*, 2010, **39**, 3240-3255.
3. J. M. Wilson, *Hum. Gene Ther.*, 2005, **16**, 1014-1015.
4. C. E. Thomas, A. Ehrhardt and M. A. Kay, *Nat. Rev. Genet.*, 2003, **4**, 346-358.
5. A. L. Barran-Berdon, S. K. Misra, S. Datta, M. Muñoz-Úbeda, P. Kondaiah, E. Junquera, S. Bhattacharya and E. Aicart, *J. Mater. Chem. B*, 2014, **2**, 4640-4652.
6. W. Qu, S.-Y. Qin, Y. Kuang, R.-X. Zhuo and X.-Z. Zhang, *J. Mater. Chem. B*, 2013, **1**, 2147-2154.
7. L. Zhang, C. Hu, Y. Fan and Y. Wu, *J. Mater. Chem. B*, 2013, **1**, 6271-6282.
8. L. Zhang, Q.-H. Yin, J.-M. Li, H.-Y. Huang, Q. Wu and Z.-W. Mao, *J. Mater. Chem. B*, 2013, **1**, 2245-2251.
9. H. Yin, R. L. Kanasty, A. A. Eltoukhy, A. J. Vegas, J. R. Dorkin and D. G. Anderson, *Nat. Rev. Genet.*, 2014, **15**, 541-555.
10. M. A. Mintzer and E. E. Simanek, *Chem. Rev.*, 2008, **109**, 259-302.
11. J. W. Yoo, D. J. Irvine, D. E. Discher and S. Mitragotri, *Nat Rev Drug Discov*, 2011, **10**, 521-535.
12. M. Zorko and U. Langel, *Adv. Drug Deliv. Rev.*, 2005, **57**, 529-545.
13. V. Bagnacani, V. Franceschi, M. Bassi, M. Lomazzi, G. Donofrio, F. Sansone, A. Casnati and R. Ungaro, *Nat. Commun.*, 2013, **4**, 1721.
14. J. Chang, X. Xu, H. Li, Y. Jian, G. Wang, B. He and Z. Gu, *Adv. Funct. Mater.*, 2013, **23**, 2691-2699.
15. K. Miyata, N. Nishiyama and K. Kataoka, *Chem. Soc. Rev.*, 2012, **41**, 2562-2574.
16. P. Xu, S. Y. Li, Q. Li, E. A. Van Kirk, J. Ren, W. J. Murdoch, Z. Zhang, M. Radosz and Y. Shen, *Angew. Chem. Int. Ed.*, 2008, **47**, 1260-1264.
17. S. Kang, K. Lu, J. Leelawattanachai, X. Hu, S. Park, T. Park, I. M. Min and M. M. Jin, *Gene Ther.*, 2013, **20**, 1042-1052.
18. X. H. Xu, H. Yuan, J. Chang, B. He and Z. W. Gu, *Angew. Chem. Int. Ed.*, 2012, **51**, 3130-3133.
19. Z. Zhang, X. Zhang, X. Xu, Y. Li, Y. Li, D. Zhong, Y. He and Z. Gu, *Adv. Funct. Mater.*, 2015, DOI: 10.1002/adfm.201502049.
20. X. H. Xu, Y. T. Jian, Y. K. Li, X. Zhang, Z. X. Tu and Z. W. Gu, *ACS Nano*, 2014, **8**, 9255-9264.
21. K. K. Ng, J. F. Lovell and G. Zheng, *Acc. Chem. Res.*, 2011, **44**, 1105-1113.

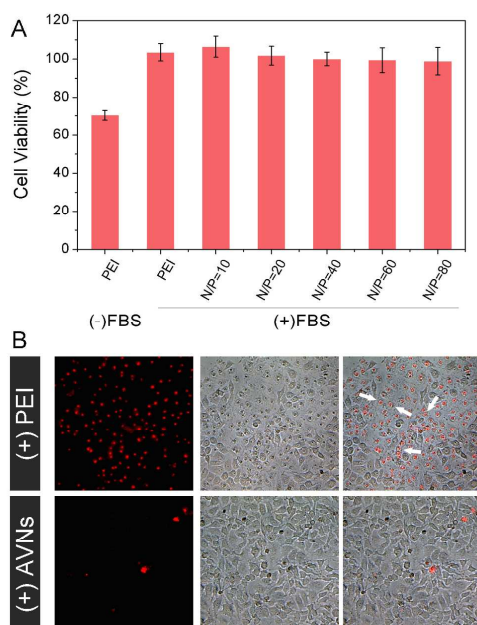


Fig 5. (A) Cell viability of HepG2 cells after exposure to the PEI/DNA complex (N/P = 10), AVNs/DNA complex (N/P from 10 to 80) for 48 h (mean \pm SD, n = 6). (B) Fluorescent field, bright field and merged image of for HepG2 cells after exposure to the PEI/DNA complex and AVNs/DNA complex with FBS for 24 hours.

Conclusions

In summary, we successfully demonstrated a facile strategy on the development of the virus-inspired nanovectors which self-assembled from the arginine-containing dendritic lipopeptides. The bioinspired nanovectors had well-defined nanostructure and strong ability for DNA condensation. Moreover, AVNs provided high efficiency, good biocompatibility and serum resistance to tumor cell lines. This demonstration indicate that combining bioinspired molecular design with supramolecular fabrication hold great promise for developing advanced gene delivery system. We are making plans to incorporate more bioinspired considerations, such as biological sensitivity and tumor-specific targeting, for in vivo and

22. X. Zhang, Z. J. Zhang, X. H. Xu, Y. K. Li, Y. C. Li, Y. T. Jian and Z. W. Gu, *Angew. Chem. Int. Ed.*, 2015, **54**, 4289-4294.
23. X. Xu, Y. Li, H. Li, R. Liu, M. Sheng, B. He and Z. Gu, *Small*, 2014, **10**, 1133-1140.
24. K. K. Ewert, H. M. Evans, A. Zidovska, N. F. Bouxsein, A. Ahmad and C. R. Safinya, *J. Am. Chem. Soc.*, 2006, **128**, 3998-4006.
25. Z. X. Zhou, Y. Q. Shen, J. B. Tang, E. L. Jin, X. P. Ma, Q. H. Sun, B. Zhang, E. A. Van Kirk and W. J. Murdoch, *J. Mater. Chem.*, 2011, **21**, 19114-19123.
26. T. Zhang, X. Song, D. Kang, L. Zhang, C. Zhang, S. Jin, C. Wang, J. Tian, J. Xing and X.-J. Liang, *J. Mater. Chem. B*, 2015, **3**, 4698-4706.
27. Y. Nie, M. Gunther, Z. Gu and E. Wagner, *Biomaterials*, 2011, **32**, 858-869.
28. H. Lv, S. Zhang, B. Wang, S. Cui and J. Yan, *J. Control. Release*, 2006, **114**, 100-109.
29. C. Riccardi and I. Nicoletti, *Nat. Protoc.*, 2006, **1**, 1458-1461.